UPTEC X 04 027
MAJ 2004

ISSN 1401-2138

MARIA WERNER

# Numerical solution to the master equation using the linear noise approximation

Master's degree project

UPPSALA UNIVERSITET

# Molecular Biotechnology Programme

Uppsala University School of Engineering

| **UPTEC X 04 027** | **Date of issue 2004-05** |
|---|---|


Author

**Maria Werner**


Title (English)

**Numerical solution the the master equation using the linear noise approximation**

Title (Swedish)


Abstract

Biological systems can be modelled stochastically *in silico* with the master equation. However, the computational demands in these calculations restrict the number of dimensions of the biological system, that is the number of species involved. In this thesis, the application of the linear noise approximation to the master equation is tested in order to simplify the computational problems. The approximation can then allow us to study systems of higher dimensions. Here, both two- and four-dimensional systems were studied and compared to earlier calculations with the master equation using the Fokker-Planck approximation.



Keywords

System biology, master equation, LNA, linear noise approximation, mesoscopic, stochastics.



Supervisors

**Paul Sjöberg**
**Department of Scientific Computing, Uppsala Universitet**

Scientific reviewer

**Per Lötstedt**
**Department of Scientific Computing, Uppsala Universitet**


| Project name | Sponsors |
|---|---|
| Language **English** | Security |
| **ISSN 1401-2138** | Classification |
| Supplementary bibliographical information | Pages **37** |


**Biology Education Centre** Biomedical Center Husargatan 3 Uppsala
Box 592 S-75124 Uppsala Tel +46 (0)18 4710000 Fax +46 (0)18 555217

# Numerical solution to the master equation using the linear noise approximation

**Maria Werner**

Sammanfattning

Intresset för att kunna studera olika biologiska system är stort och har varit under mycket lång tid. Idag kan vi med hjälp av olika molekylärbiologiska metoder studera olika typer av system som t.ex. uttryck av gener eller enzymatiska reaktioner som sker i kroppen. Det är dock fortfarande svårt att laborativt undersöka mycket små system, något som lett till utvecklingen av matematiska beskrivningar samt datasimuleringar som komplement till den laborativa forskningen.

Ett vanligt sätt att beskriva enkla enzymatiska reaktioner teoretiskt är att använda sig av ordinära differentialekvationer. Men om man vill modellera ett system med endast ett fåtal molekylslag så krävs att man använder andra matematiska beskrivningar som tar hänsyn till sannolikheterna för varje molekyl att reagera. Master ekvationen är en sådan beskrivande modell som vid lösning ger en sannolikhetsfördelning för hur systemet ser ut över tiden. Dock leder denna stokastiska beskrivning till att beräkningsbelastningen ökar exponentiellt för varje involverat molekylslag, och stora system blir i praktiken omöjliga att studera.

I detta projekt har ett litet system med två till fyra molekylslag studerats teoretiskt med hjälp av master ekvationen. Ekvationen har lösts numeriskt i MATLAB genom användning av den så kallade linjära störningsapproximationen. Denna approximation leder till en uppdelning av master ekvationen i två delar, en deterministisk del med differentialekvationer, och en stokastisk del som genererar en sannolikhetsfördelning. En sådan uppdelning resulterar i en minskad beräkningsbelastning för stora system, och gör det lättare att kunna genomföra datasimuleringar på dessa.

**Examensarbete 20 p i Molekylär bioteknikprogrammet**

**Uppsala Universitet maj 2004**

# Contents

# 1 Introduction

There is a great need for understanding how different biological systems work, from small cellular systems to large population systems. At the same time it can be difficult to study these systems isolated and correctly. Population studies may be difficult regarding time and isolation, and the study of cellular systems can be difficult due to the need for exact measurement techniques. Using mathematical models to describe variations of reactants over time in a cell is now an alternative approach available for scientists.

The simplest way of describing a cellular system mathematically is with differential equations for changes in concentrations of the involved reactants. These equations are possible to solve easily with computers but they give a limited view of the system and they can give misleading solutions when dealing with certain biochemical systems. A more accurate model can be created based on the stochastic master equation. This equation gives a total description of the system using the stochastics of each reaction. The stochastic nature of a system is of great importance in cases where the involved reactants are present in low copy numbers, making it misleading to speak about mean concentrations. Calculations with this approach is the solution to studying many cellular systems, but it is more computationally demanding.

In this project the goal is to solve the master equation numerically using the linear noise approximation described by van Kampen in *"Stochastic processes in physics and chemistry"* [2]. The method is based on expanding the equation in a variable, $\Omega$, relevant in the description of the stochastics of the system. The expansion leads to a separation of the master equation into two parts, one deterministic and one stochastic. A dimensionality reduction of the stochastic part is possible to perform, lowering the computational demands for the system solving. This approach can hopefully lead to possibilities of studying larger systems with a stochastic view.

# 2 Background

The study of biological systems has been of interest to mankind throughout the greater part of our history. Today we are able to study systems that were impossible 50 years ago and the increasing computational abilities that are present for today's scientists, can hopefully lead to an expansion of the range of possible systems to study.

There is a large number of molecular systems in our bodies that are of great interest to study in detail. Knowledge about for example metabolic flows and their control systems gives us an opportunity to understand different diseases and the possibility to discover a way to treat them. Intracellular processes are of especially great importance since they include regulation of gene expression, the most fundamental instructions for the body. Several of the intracellular processes are however very complex, meaning involving a large number of enzymes, co-enzymes and regulators. To build models of these systems is a big challenge. More easily studied systems are isolated enzyme turnovers, with just a few molecules involved. The most common way to describe these systems is by using differential equations, displaying the variations of mean concentrations for the reactants involved.

This project involves performing calculations on systems with only a few molecular species involved. But instead of using simple differential equations the systems will be described stochastically, using the linear noise approximation of the master equation, in order to get a more accurate description. Solving the master equation numerically has been performed earlier by P. Sjöberg in his master thesis [1], with the Fokker-Planck approximation for the master equation. In this project, the results will be compared with results from Sjöberg's project. The mathematical theories behind the linear noise approximation are described by N.G. van Kampen in [2].

It is impossible to study an isolated part of a biological system and from its behavior obtain a total understanding of the whole system. A cell for example, is a system which is built up of many different compartments with different tasks and regulatory systems. Just investigating one of these compartments and finding its role does not in any way give us a clear picture of the function of the whole cells.

The goal of this project is therefore not to analyze the molecular system that is described and draw conclusions about mechanisms that operate on higher levels in the cell. The goal is to try a method of numerically solving the mathematical description of a system that are based on reactions taking place inside a cell. Hopefully though, in time, it will be possible to study even larger systems than what is done here, which might explain mechanisms in the cell that were unknown before.

In the following sections the possible ways of describing a system mathematically will be presented together with a presentation of the molecular systems used in this project.

## 2.1 Macroscopic and mesoscopic views

Chemical reactions are usually described macroscopically, using mean concentrations of the reactants involved to describe the system's variations. The system can then vary continously over time. This is a correct description of a system where the reactants exist in a large amount over all times, large enough to make small fluctuations irrelevant. However, the biochemistry going on in our cells often involves molecules present in low copy numbers, sometimes as low as only a few molecules. The relative variance of the concentrations in these systems can then become very large, meaning the fluctuations of the system are highly relevant for its dynamics.

A macroscopic model uses differential equations to describe the system's evolution over time. Differential equations are deterministic and will therefore always evolve in the same way, regardless of the system's initial state. They display the change of mean concentrations over time. However, in systems where molecules are present in a very low copy number, the discrete number of involved molecules becomes more important than the average. A fluctuation in the copy number is then of great importance for the probability of a reaction to occur. These fluctuations are not shown when solving equations based on the average concentrations, implying that in order to get a relevant solution there is a need for an alternative view on the system: the mesoscopic view.

The mesoscopic view of studying a system is necessary for handling fluctuations in the system. Fluctuations is a property of the system caused by the fact that it consists of discrete particles. This noise can never disappear from the

system, only be neglected. Neglecting the fluctuations leads to the macroscopic approximation of a system, thus originating from the mesoscopic model [2].

With a mesoscopic view a reaction occurs with a certain probability. Each process is stochastic and the probabilities for all reactions are studied together with the probabilities of being in different states. The system dynamics is solved with the master equation giving the probability distribution for the system's states over time. This distribution is also the distribution for a population of cells, where the individual cell can change states but the total distribution will remain the same.

## 2.2 The modeling of a system

When trying to model a system of any kind, one needs to find a set of parameters that altogether can give the necessary information about the system. In biological systems these parameters usually consist of the reactants involved, their concentrations and the rates with which the possible reactions take place. This way of modeling systems is the one we are taught in school when we first start to study chemistry. In mesoscopic models the parameters are slightly different but the base is the same. The differences and the similarities between these two types of models will be presented here in this section.

In the macroscopic way of modeling, chemical reactions are often displayed in the following way:

$$Y + X \xrightarrow{k} Z,$$

where $k$ is the reaction rate and $X$, $Y$ and $Z$ are the concentrations of the different reactants. This reaction describes the building of a third molecule out of two starting molecules. Differential equations can from here be constructed where the change of concentrations is described by the reaction rate $k$. Often in biology, one talks about steady states. A steady state is a state for the system where its inflows and outflows are equal, i.e. there is no change of concentration for the reactants. Solving the differential equations for the mean-concentrations of reactants will reveal if there exists a steady state for the system.

In mesoscopic calculations a reaction is described as a transition between two states and reactions that *in vivo* are bidirectional are here presented as two separate transitions, each unidirectional. Mesoscopic calculations involves working with the probabilities for the system to change through its predefined reactions. A transition takes the system from one state to another with a certain probability. The state of the system is defined by its present amount, $x_i$, of each reactant $i$, $\mathbf{x} = \{x_1, x_2, , \ldots, x_d\}$. A system with $d$ reactants, each of dimension $n$, can be in $n^d$ different states. The dimension $n$ is the range of molecule $d$ in the model. In real life the range goes to infinity, but in a model it is necessary to restrain $n$, that is to truncate the system. The number of states being $n^d$ will of course lead to an exponential increase in the number of states with each added reactant. The probabilities of all these states need to be calculated, explaining the difficulties for performing simulations on large systems using the mesoscopic approach.

The mesoscopic way of writing the same reaction presented above would be:

$$\begin{aligned} \mathbf{x}_r &\xrightarrow{w_r(\mathbf{x}_r)} \mathbf{x} \\ \mathbf{n}_r &= \mathbf{x}_r - \mathbf{x}, \end{aligned} \tag{2}$$

where $w_r$ is the transition probability per unit time from state $\mathbf{x}_r$ to state $\mathbf{x}$ and $\mathbf{n}_r$ is the change in molecules between state $\mathbf{x}_r$ and state $\mathbf{x}$. The state is here represented by the number of $x$, $y$ and $z$ present in the system:

$$\begin{aligned} \textit{state } \mathbf{x}_r &= \{x, y, z\} \\ \textit{state } \mathbf{x} &= \{x-1, y-1, z+1\} \\ \textit{step } \mathbf{n}_r &= \{1, 1, -1\}, \end{aligned}$$

where $x$, $y$ and $z$ are number of molecules, not their concentrations.

The transition probability per unit time originates from the reaction rates and multiplied with the probability of being in state $\mathbf{x}_r$ it gives the probability flow from $\mathbf{x}_r$ to $\mathbf{x}$. The correlation between reaction rates and transition probabilities is fairly direct. To illustrate this an example of reactions and transitions and their corresponding rates and probabilities is given in table 1. The example is one of the systems that are studied in this project.

Solving the master equation is the way of studying a system with a mesoscopic view. This equation is based on probabilities of being in states and to jump between them. Knowledge about all probability flows throughout the system gives the necessary information for solving the master equation, resulting in the probability distribution for the system over time. This probability distribution displays the dynamics of the system. Further details on the master equation and its structure and solving are presented in the theory and method sections.

## 2.3 The biological system

In the cells, genes are expressed through the ribosomes that translate the genetic code into peptide sequences, forming the primary structure of the proteins. There are 20 different amino acids present in the cells, each synthesized by a special enzyme. About $10^4$ amino acids have to be synthesized every second, in each cell, in order to produce all the necessary proteins [9]. This requires a strict and efficient control system, regulating the production of amino acids and balancing the concentrations so there are no limitations of certain amino acids which could lead to an increase in substitution errors in the protein structure [11].

If the turnover rate, the rate with which the molecules are produced and consumed, is much higher than the dilution rate, there will be large fluctuations in the amino acid pool inside the cell [8]. This implies that the system should be studied with a mesoscopic view rather than a macroscopic. In this project the systems used are general models but they are based on the type of reactions occurring in for example amino acid regulation. Amino acids are produced, then coupled to their tRNA and consumed through an irreversible reaction where the aminoacyl-tRNAs are used by the ribosome. The systems modeled here are very limited, concerning only the involved reactants and regarding the rest of the cell as a source and sink from which they are produced and consumed back into. In the report the molecular species will be denoted with capital letters, $A$ and $B$. Their concentrations are referred to as $[a]$ and $[b]$ and the number of molecules, $a$ and $b$.

The first system models two aminoacyl-tRNAs, $A$ and $B$, forming separately and being consumed through dilution and a bimolecular reaction forming a third complex. The second system is four-dimensional and includes, besides molecules $A$ and $B$, the two enzymes $E_A$ and $E_B$ involved in the production of the amino acids, $A$ and $B$. The two synthetases $E_A$ and $E_B$ are controlled using feedback inhibition through a repressor molecule $R$. This is a common regulation mechanism in biochemical systems where a large concentration of a product leads to a lower expression of its synthetase [6]. In the models we neglect the diffusion that is present in almost any systems *in vivo*. We assume that the diffusion is much faster than the reactions, resulting in homogeneity of the system. The systems modelled here are based on studies of aminoacidregulations in *Escherichia coli*. An example of reactions and transitions for the two-dimensional system is given in table 1 and details about the reactions and the constants used are given for the two systems in appendix A.

Table 1: The correlation between macroscopic and mesoscopic descriptions. The transition probabilities are based on the reaction rate for the corresponding reaction and simply converted to the unit $s^{-1}$. The constants involved in this system have different unit to start with, $k_0$ in $Ms^{-1}$, $\mu$ in $s^{-1}$ and $k_2$ in $M^{-1}s^{-1}$. The $\emptyset$ denotes the source and sink.

| reaction | reaction rates $[Ms^{-1}]$ | transition prob. $[s^{-1}]$ | transition |
|---|---|---|---|
| $\emptyset \xrightarrow{k_0} A$ | $k_0$ | $\Omega k_0$ | $\{a,b\} \to \{a+1,b\}$ |
| $\emptyset \xrightarrow{k_0} B$ | $k_0$ | $\Omega k_0$ | $\{a,b\} \to \{a,b+1\}$ |
| $A \xrightarrow{\mu[a]} \emptyset$ | $\mu[a]$ | $\Omega\mu[a]$ | $\{a,b\} \to \{a-1,b\}$ |
| $B \xrightarrow{\mu[b]} \emptyset$ | $\mu[b]$ | $\Omega\mu[b]$ | $\{a,b\} \to \{a,b-1\}$ |
| $A+B \xrightarrow{k_2[a][b]} \emptyset$ | $k_2[a][b]$ | $\Omega k_2[a][b]$ | $\{a,b\} \to \{a-1,b-1\}$ |

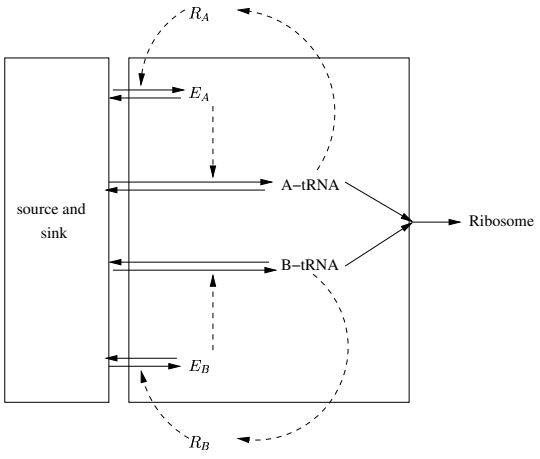


Figure 1: The figure illustrates a scheme over the four-dimensional system schematically written. The t-RNA $A$ and $B$ together with the enzymes $E$ and their regulators $R$. Solid lines describe production and consumption through reactions while dotted lines indicates influences on these reaction rates.

# 3 Theory

The model used in this thesis is based on the so-called expansion theory of van Kampen [2], also known as the linear noise approximation, LNA. In order to explain this model one needs to understand the theory behind it, namely the master equation and the Fokker-Planck approximation of the former.

## 3.1 The master equation

The master equation is a linear, time-dependent equation for the probability density of the chemical species in a system. If there exists $d$ different species in the system to be modeled, the equation will be $d$-dimensional. The master equation originates from Markov processes, processes that by definition are stochastic and where the transition probability only is dependent on the current state, not of earlier states or transitions. For a system with a discrete number of particles the equation is discrete in space.

The dynamics of a system is based on its defined reactions. Each macroscopic reaction in the system has a corresponding mesoscopic probability flow, as seen in table 1. The total probability flow for a certain state is the sum of all probability flows, to and from that state. Summarizing flows over all states and time gives a system of linear, time-dependent difference equations, the master equation:

$$\begin{aligned}\frac{\partial p(\mathbf{x},t)}{\partial t} &= \sum_{r=1}^{R} w_r(\mathbf{x}+\mathbf{n_r})p(\mathbf{x}+\mathbf{n_r},t) - \sum_{r=1}^{R} w_r(\mathbf{x})p(\mathbf{x},t) \\ &= \sum_{r=1}^{R} \Big( q_r(\mathbf{x}+\mathbf{n_r},t) - q_r(\mathbf{x},t) \Big)\end{aligned} \tag{3}$$

As mentioned before, the transition probability per unit time, $w_r(\mathbf{x})$ multiplied by the probability of being in state $\mathbf{x}$, $p(\mathbf{x},t)$ gives the probability flow from state $\mathbf{x}$, $q_r(\mathbf{x},t)$. Likewise, $w_r(\mathbf{x}+\mathbf{n_r})p(\mathbf{x}+\mathbf{n_r},t)$ gives the probability flow toward state $\mathbf{x}$ from state $\mathbf{x}+\mathbf{n_r}$. The solution to the master equation is the probability distribution, $p(\mathbf{x},t)$. This distribution is time-dependent and displays the probability for the system of being in the different possible states.

## 3.2 The Fokker-Planck approximation

The master equation can be approximated by the Fokker-Planck equation [2]. This approximation is a Taylor expansion around the state $\mathbf{x}$, truncated after the second derivative, and gives a continuous approximation of the flows between states. One can perform the Taylor expansion in different ways. Here the total probability flow $q_r(\mathbf{x}+\mathbf{n_r})$ is expanded, not only $w_r(\mathbf{x}+\mathbf{n_r})$. The resulting Fokker-Planck approximation is shown below,

$$\frac{\partial p(\mathbf{x},t)}{\partial t} \approx \sum_{r=1}^{R} \Big( \mathbf{n_r} \nabla_x (w_r(\mathbf{x}) p(\mathbf{x},t)) + 0.5 \mathbf{n_r} \mathcal{H}(w_r(\mathbf{x}) p(\mathbf{x},t)) \mathbf{n_r} \Big)$$
$$= \sum_{r=1}^{R} \Big( \sum_{i=1}^{d} n_{ri} \frac{\partial (w_r(\mathbf{x}) p(\mathbf{x},t))}{\partial x_i} + \sum_{i=1}^{d} \sum_{j=1}^{d} \frac{n_{ri} n_{rj}}{2} \frac{\partial^2 (w_r(\mathbf{x}) p(\mathbf{x},t))}{\partial x_i x_j} \Big), \tag{4}$$

where $\nabla_x$ are the derivatives of first order and $\mathcal{H}$ is the Hessian matrix consisting of second order derivatives. $R$ is the number of reactions involved in the system with $n_{ri}$ as the change for molecule $i$ between the old state and the new state, changed through reaction $r$, and $d$ is the number of reactants present in the system.

The equation is discretized using difference approximations. The system of equations can thereafter be described by a system matrix $A$, containing all the derivative approximations of the probability flows throughout the system. The derivative approximations and the grid are described further in the method section.

### 3.3 Linear noise approximation

Using the Fokker-Planck approximation when solving the master equation reduces the system of equations. But the dimensionality problems remain. For every reactant, the problem adds a dimension and the system matrix $A$ becomes large. Despite the capacities of today's computers, there is a need for finding a way of solving these stochastic multidimensional equations with a different approach. An alternative method for approximating the master equation, that might be the solution to the dimensionality problem, is the linear noise approximation [2]. This approximation method concerns the stochastic variations of the involved reactants and an elimination of variables leading to a problem with lower dimensionality.

The LNA is an approximation of the master equation and is therefore a mesoscopic view of modeling. If $\phi_i$ is an average concentration of a reactant in a system, the number of molecules of the same reactant, $x_i$, is expected to be $x_i = \Omega\phi_i$, where $\Omega$ is the volume of the system. The deviation from $x_i$ is expected to be of order $x_i^{\frac{1}{2}}$, and the effect they have on the macroscopic properties of the system will be of order $x_i^{-\frac{1}{2}}$ [2]. The parameter $\Omega$ is consequently of importance measuring the fluctuations relative to the concentrations. Expanding the systems all variables in orders of $\Omega$ gives a description of the system on two different levels, the macroscopic and the mesoscopic. Using $\Omega$ as an expansion variable will be possible after performing a change of variables for the reactants. The amount of each reactant $x_i$ is therefore replaced with a set of two variables;

$$x_i = \Omega\phi_i + \Omega^{\frac{1}{2}}\xi_i, \tag{5}$$

where $\phi_i$ is the mean concentration of reactant $i$ and $\xi_i$ is the deviation for reactant $i$ from $\phi_i$. The deviation is here a linear term, hence the name linear noise approximation.

In van Kampen's method $\Omega$ is referred to as a parameter chosen so that for large $\Omega$ the changes between states are relatively small. $\Omega$ is chosen to be the base of the expansion since it is a parameter that already exists in the master equation, and it is of great relevance for the stochastics of the system. With $\Omega$ going to infinity the fluctuations will become insignificant and the system can be modeled macroscopically.

Changing the variables of the involved reactants means also changing the function $p(\mathbf{x}, t)$ to a function $\Pi(\bar{\phi}, \bar{\xi}, t)$, with $\bar{\xi} = \{\xi_1, \xi_2 \ldots, \xi_d\}$ being the vector containing all stochastic variables, and $\bar{\phi} = \{\phi_1, \phi_2 \ldots, \phi_d\}$ being the vector containing all mean concentration parameters for the system. The purpose of the expansion model is to rewrite the master equation in the new variables giving it a structure that is defined by orders of $\Omega$ and therefore separable. In the following section, the general expansion model will be presented and for more details see appendix B where a two-dimensional example is given.

### 3.3.1 The general expansion and separation

In this section, the master equation will be rewritten with the linear noise approximation, formulating two new separate equations, in new variables. The whole approximation is based on expanding variables in powers of $\Omega$, including these in the master equation and perform a separation of scales, yielding two equations instead of one. Starting the approximation, all concentrations of involved reactants are expressed in powers of $\Omega$ according to (5). The distribution function $p(x, t)$ will after this variable change be a function of $\xi$ and $t$, $\Pi(\xi, t)$.

$$\begin{aligned} p(x_1, x_2, \ldots x_d, t) &= p(\Omega\phi_1 + \Omega^{\frac{1}{2}}\xi_1, \Omega\phi_2 + \Omega^{\frac{1}{2}}\xi_2, \ldots, \Omega\phi_m + \Omega^{\frac{1}{2}}\xi_d, t) \\ &= \Pi(\xi_1, \xi_2, \ldots, \xi_d, t). \end{aligned} \tag{6}$$

where $\phi_i$ are mean concentrations and are assumed to only depend on time. The different orders of $\Omega$ are expressed through the variable changes in the probability flows seen in (8).

The probability flow $q_r$, from state $\mathbf{x} + \mathbf{n_r}$ to state $\mathbf{x}$ is rewritten in the new variables as well:

$$\begin{aligned} w_r(\mathbf{x} + \mathbf{n_r})p(\mathbf{x} + \mathbf{n_r}, t) &= q_r(\mathbf{x} + \mathbf{n_r}, t) \\ &= q_r(\Omega\bar{\phi} + \Omega^{\frac{1}{2}}\bar{\xi} + \mathbf{n_r}, t) \\ &= q_r(\Omega\bar{\phi} + \Omega^{\frac{1}{2}}(\bar{\xi} + \Omega^{-\frac{1}{2}}\mathbf{n_r}), t) \\ &= \rho_r(\bar{\xi} + \Omega^{-\frac{1}{2}}\mathbf{n_r}, t), \end{aligned} \tag{7}$$

The last equality, resulting in the function $\rho_r(\bar{\xi}, t)$, arises since $\bar{\phi}$ is only a function of $t$, $\bar{\phi}(t)$. The probability flow $\rho_r$ now contains the different orders of $\Omega$ in its new definition:

$$\begin{aligned} \rho_r(\xi, t) &= \omega_r(\xi, t)\Pi(\xi, t) \\ \omega_r(\xi, t) &= \textstyle\sum_{k=0}^{l} \Omega^{1-\frac{k}{2}}\omega_{rk}(\xi, t). \end{aligned} \tag{8}$$

Each $w_r$ that before was the probability flow for the total transition, is now separated into a sum of several $\omega_{rk}$, a Taylor expansion in $\Omega^{-\frac{1}{2}}$. This sum can

be finite or infinite depending on the structure of $w_r$. The new $\omega_{rk}$ are simply the result of the variable change from one variable, $x$, to two variables $\bar{\phi}$ and $\bar{\xi}$. The index $k$ indicates which order of $\Omega$ the flow describes. For an example see appendix B.

Finding the mathematical relationship between the two probability distributions is done through simple derivation of $p(\mathbf{x}, t)$ with respect to $t$. Using the function $\rho_r$ together with this relationship, the master equation can be reformulated:

$$\frac{\partial p(\mathbf{x},t)}{\partial t} = \frac{\partial \Pi}{\partial t} - \sum_{i=1}^{m} \Omega^{\frac{1}{2}} \frac{d\phi_i}{dt} \frac{\partial \Pi}{\partial \xi_i}$$

$$\begin{aligned}
\frac{\partial \Pi(\bar{\xi},t)}{\partial t} - \sum_{i=1}^{m} \Omega^{\frac{1}{2}} \frac{d\phi_i}{dt} \frac{\partial \Pi}{\partial \xi_i} &= \sum_{r=1}^{R} \Big( \rho_r(\bar{\xi} + \Omega^{-\frac{1}{2}} \mathbf{n_r}, t) - \rho_r(\bar{\xi}, t) \Big) \\
&\approx \sum_{r=1}^{R} \Big( \Omega^{-\frac{1}{2}} n_r \nabla_\xi \rho_r(\bar{\xi}, t) + \frac{1}{2} \Omega^{-1} n_r \mathcal{H}(\rho_r(\bar{\xi}, t)) n_r \Big) \\
&= \sum_{r=1}^{R} \Big( \Omega^{-\frac{1}{2}} \sum_{i=1}^{d} n_{ri} \frac{\partial \rho_r(\bar{\xi}, t)}{\partial \xi} + \Omega^{-1} \sum_{i=1}^{d} \sum_{j=1}^{d} \frac{n_{ri} n_{rj}}{2} \frac{\partial^2 (\rho_r(\bar{\xi}, t))}{\partial \xi_i \partial \xi_j} \Big)
\end{aligned} \tag{9}$$

The Taylor expansion performed here, with $\mathbf{n_r}$ defined as in (2), corresponds to the Fokker-Planck approximation, (4), but now in the new variables. Using the probability flows from (8) together with the approximated master equation, (9), the resulting stochastic equation can be written:

$$\begin{aligned}
\frac{\partial \Pi}{\partial t} - \Omega^{\frac{1}{2}} \sum_{i=1}^{m} \frac{d\bar{\phi}_i}{dt} \frac{\partial \Pi}{\partial \xi_i} &\approx \sum_{r=1}^{R} \Big( \Omega^{-\frac{1}{2}} \sum_{i=1}^{d} n_{ri} \frac{\partial \rho_r(\xi, t)}{\partial \xi_i} + \Omega^{-1} \sum_{i=1}^{d} \sum_{j=1}^{d} \frac{n_{ri} n_{rj}}{2} \frac{\partial^2 (\rho_r(\xi, t))}{\partial \xi_i \partial \xi_j} \Big) \\
&= \sum_{r=1}^{R} \Big( \Omega^{-\frac{1}{2}} \sum_{i=1}^{d} \sum_{k=0}^{l} n_{ri} \Omega^{1-\frac{k}{2}} \frac{\partial (\omega_{rk} \Pi)}{\partial \xi_i} \\
&\quad + \Omega^{-1} \sum_{i=1}^{d} \sum_{j=1}^{d} \sum_{k=0}^{l} \Omega^{1-\frac{k}{2}} \frac{n_{ri} n_{rj}}{2} \frac{\partial^2 (\omega_{rk} \Pi)}{\partial \xi_i \partial \xi_j} \Big) \\
&= \Omega^{\frac{1}{2}} \sum_{r}^{R} \sum_{i}^{d} n_{ri} \frac{\partial (\omega_{r0} \Pi)}{\partial \xi_i} + \Omega^0 \sum_{r}^{R} \sum_{i}^{d} n_{ri} \frac{\partial (\omega_{r1} \Pi)}{\partial \xi} + \mathcal{O}(\Omega^{-\frac{1}{2}}) \\
&\quad + \Omega^0 \sum_{r}^{R} \sum_{i}^{d} \sum_{j}^{d} \frac{n_{ri} n_{rj}}{2} \frac{\partial^2 (\omega_{r0} \Pi)}{\partial \xi_i \partial \xi_j} + \mathcal{O}(\Omega^{-\frac{1}{2}})
\end{aligned} \tag{10}$$

Equation (10) describes the derivative of the probability function $\Pi(\xi, t)$ expressed in powers of $\Omega$. There is a summation over all involved reactions, $R$, and over all involved reactants, $d$. Since $\Omega$ has a relatively large value, all the

terms of lower order than $\Omega^0$ are neglected and left are only the terms of order $\Omega^0$ or $\Omega^{\frac{1}{2}}$. These terms can be separated due to the large difference in scales:

$$\Omega^{\frac{1}{2}}: \quad 0 = \sum_{i=1}^{d} \frac{d\phi_i}{dt} \frac{\partial \Pi}{\partial \xi_i} + \sum_{r=1}^{R} \sum_{i=1}^{d} n_{ri} \frac{\partial}{\partial \xi_i} (\omega_{r0} \Pi) \tag{11}$$

$$\Omega^0: \quad \tfrac{\partial \Pi}{\partial t} = \sum_{r=1}^{R} \sum_{i=1}^{d} n_{ri} \frac{\partial}{\partial \xi_i} (\omega_{r1} \Pi) + \frac{1}{2} \sum_{r=1}^{R} \sum_{i=1}^{d} \sum_{j=1}^{d} n_{ri} \frac{\partial}{\partial \xi_i \partial \xi_j} n_{rj} (\omega_{r0} \Pi) \tag{12}$$

Since $\omega_{r0}$ is a function of time only, following from the expansion, this gives:

$$\sum_{i=1}^{d} \Big( \frac{d\phi_i}{dt} + \sum_{r=1}^{R} n_{ri}(\omega_{r0}) \Big) \frac{\partial \Pi}{\partial \xi_i} = 0$$

and for this to hold for all $\Pi$:

$$\frac{d\phi_i}{dt} + \sum_{r=1}^{R} n_{ri}(\omega_{r0}) = 0. \tag{13}$$

The master equation has now, by changing parameters and separating the equation by means of orders of $\Omega$, become two equations. The $\phi$-terms in (10) are all of an order $\Omega^{\frac{1}{2}}$ larger than the terms with $\xi$, making the separation possible. The first system of equations, (11), with orders of $\Omega^{\frac{1}{2}}$ has the form of a differential equation with the variable $\bar{\phi}$. The second, (12), is a Fokker-Planck equation with $\Pi(\bar{\xi}, t)$ instead of $p(\mathbf{x}, t)$ [2]. Both equations describe the system dynamics but on different scales. The differential equation system display the larger changes over time, the mean-concentration variations of the reactants, while the stochastic equation display the fluctuations. Both equations have to be solved in order to correctly model the time evolution of the system.

For systems that are multidimensional, the linear noise approximation can be difficult to solve numerically. It is even more demanding than solving the Fokker-Planck approximation since the system matrix $A$ now is time-dependent, as discussed in the method section. However, in larger systems it may not be necessary to study the stochastics of every involved reactant. Some may be present in a much larger copy number than others, making their fluctuations less relevant to model. The LNA can then be applied solving the macroscopic changes for all the reactants, but restricting the stochastic part to only those reactants with larger relative fluctuations. In this report a two-dimensional system is described with stochastics of both the involved reactants. A four-dimensional problem is also studied, where only two of the reactants are mathemathically described with stochastics.

### 3.3.2 Elimination of fast variables

There is a way to make the linear noise approximation more accurate than what is presented so far in this report. Elf et al. describe in several articles the practise of elimination of fast variables, leading to a more accurate description of

the system dynamics than applying LNA directly to the system [4, 10]. The method involves a change of variables before applying LNA to the system. The variable change requires that the slow variables are linear combinations of the original concentrations and that the fast variables are at their steady state values, conditional on the slow variables [4].

In this project, this elimination method has been applied only to the two-dimensional problem. Here the new variables used in the LNA calculations are $U = A - B$ and $V = A + B$. This variable change results in $V$ containing all non-linear tendencies in the system and $U$ described only through linear equations. The eigenvalues of the system will remain the same as in the $AB$-system but the eigenvectors are now directed along the $U$ and $V$-axes, while in the $AB$-system they have 45 degree angles to the $A$ and $B$ axes, see appendix B. Therefore the fast eigenvalue now corresponds to the changes in $V$-molecules and the slow eigenvalue corresponds to the changes in $U$-molecules.

This results in $V(t)$ quickly adjusting to a quasi steady state conditional on $U$, while $U(t)$ on the other hand adjusts relatively slowly compared to $V$ [10]. A separation of timescales can then be used, applying the linear noise approximation for one variable at a time. The two different linear stochastic equations that are used is presented together with the two differential-equations in appendix B

When LNA first is performed for the $U$-variable, $V$ is fixed at its quasi steady state value.

$$V^s(U) = -\frac{\mu}{k_2} \pm \sqrt{\frac{\mu^2}{k_2^2} + \frac{4k_0}{k_2} + U^2} \tag{14}$$

The resulting probability distribution, $\Pi(\xi_U(V^s), t)$ is a one-dimensional, Gaussian distribution centered around $U = 0$ [2]. The two-dimensional probability distribution, $\Pi(U, V, t)$, can be calculated using LNA in only the $V$-variable for all $U$, with $\Pi(U(V^s))$ already determined;

$$\Pi(U, V, t) \approx \Pi((V|U), t)\Pi(U(V^s), t)$$

# 4 Programs and numerical methods

The implementation of this theory is carried out in MATLAB. The programs constructed were based on the corresponding programs by P. Sjöberg, for solving the Fokker-Planck equation numerically. The programs and methods used in this project are described shortly in this section and for further details see Sjöberg's M.Sc thesis [1].

## 4.1 Computational grids and approximations

### 4.1.1 System grid

The original biological system is truncated when defining the dimensions $n$ of the involved molecules. This truncation gives the state space for the model of the system. The state space is then discretized by defining the number of gridpoints in each dimension, setting up the total grid. The number of grid-points chosen can be less than the number of actual states. The grid-points are used for approximating the probability flows in the system, meaning that fewer grid-points give less computationally demanding equations.

To limit the computational costs, the grid needs to be restricted down to consisting of the lowest number of grid-points possible to give a numerically good approximation of the system. As will be presented further on in the report, the number of grid-points have a great impact on the computational costs for a system. The grid can be equidistant or use exponentially distributed grid-points. However, for each transition the relative change to the system is greater if the number of molecules is low. Therefore setting up the grid with exponential axes is preferred, with a higher density of grid-points in the low values.

### 4.1.2 Difference approximations

The master equation concerns computations with transitions between states in the system. The Fokker-Planck approximation and the LNA also concerns computations with transitions, but only for the grid-points chosen in the grid. The states have been approximated by a number of grid-points when defining the grid. As shown in (4), the information of interest is the first and second order derivatives of all probability flows. In the equation these are continuous but are discretized using the differential approximations with the grid-points.

Approximations of derivatives can be performed in several ways. In this project central approximations have been chosen both for the first and second order derivatives. Figure 2 illustrates the stencil used for the first and second order derivative in one dimension and figure 3 illustrates the stencils for the second order derivative in two dimensions. For exact details of the weights of the approximations see appendix C.

Since the system is restricted in the molecular space, there has to be boundary conditions for the system. Here, these consist of setting the probability of being at a boundary state equal to zero. Hence there can be no flow inwards from a state on any of the boundaries. In the simulations performed here, the grid is chosen large enough for these conditions to be fulfilled.

Figure 2: The figures illustrate the stencil used for the central differential approximations of first and second order in one dimension. The black grid-point is the one where the derivative is evaluated.

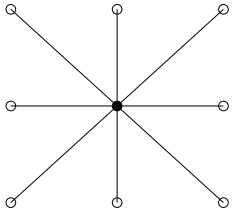

Figure 3: Illustration of the stencil used for the differential approximations of second order in two dimensions. The black grid-point is the one where the derivative is evaluated.

## 4.2 Program structure

The programs consists of several different functions in separate files. These functions are used indirectly or directly by a main-program that coordinates the iterative process of solving the distribution over a chosen time-interval. The three most important functions involved are listed in table 2 and an overview of the program structure is presented in figure 4.

Table 2: The most central functions in the program constructed for solving the master equation numerically with the linear noise approximation.

| functions | description |
|---|---|
| $[\phi] = Solve(\phi 0, \phi 1, t, dt)$ | Uses a backward difference method to calculate the concentration vector $\bar{\phi}$ at the time wanted. $\bar{\phi}0$, $\bar{\phi}1$ are mean concentrations from two earlier timesteps,$t$ is the number of timesteps used and $dt$ the lenght of each timestep. |
| $[A] = A(x\_ax, y\_ax, \bar{\phi}(t))$ | Returns the system matrix $A$. $x_{ax}$ and $y_{ax}$ are the two axis defining the state space and $\bar{\phi}$ is the mean concentration vector. |
| $[p] = BDF(A, p0, p1, dt)$ | Uses a backward difference method to calculate the distribution $p$ at the time wanted. $A$ is the system matrix, $p0$ and $p1$ probability distributions for two earlier timesteps and $dt$ the lenght of each timestep. |

Solving only the Fokker-Planck equation, as has been done as a reference in this study, there is no separation of concentration parameters and the distribution function. The distribution itself then contains information about the average concentrations in the system. Therefore it is only necessary to solve the distribution function, $p(\mathbf{x}, t)$, over time with a numerical method.

In the linear noise approximation, there is a separation between the concentrations and the noise, the disturbance from the mean-concentration, as described in the theory. The original equation was separated into differential equations describing the macroscopic mean-concentrations of the reactants, and a linear Fokker-Planck equation describing the distribution of noise over time. Solving this new Fokker-Planck equation will then only display the distribution of the variance from the steady state concentrations. The mean-concentrations of the reactants and the noise distribution are therefore needed to be solved separately.

The three large functions used in the programs will be presented here in the following sections.

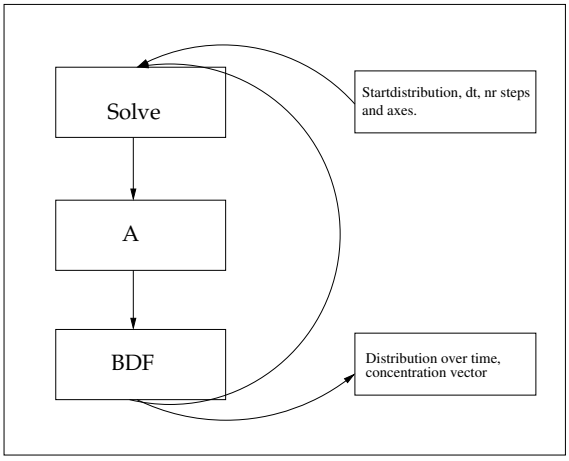


Figure 4: The structure of the main program with the stochastic part and the deterministic part solved separately. The startdistribution and start mean values are given as input. Solve is a function that calculates the mean concentration values for wanted timestep. The function A generates the system matrix A and the BDF function solves the stochastic equation for wanted timestep.

## 4.3 System matrix

The system matrix, $A$, contains all the information concerning the fluctuations of the system, i.e. it is constructed from the derivatives of the probability flows defining the system. It depends on the macroscopic solution and is time-dependent for the LNA. Starting with the distribution $\Pi(\bar{\xi}, t)$, the time evolution of this distribution can be found by:

$$\frac{d\Pi}{dt} = A\Pi \tag{15}$$

The size of $A$ is determined by the number of grid-points chosen to represent the states. If the number of points in each dimension is $N$ then the total number of states in the system will be $s = N^d$, $d$ being the number of reactants, and the size of $A$ will be $s \times s$. Fortunately, the flow into a state can only come from a limited number of adjacent states, giving the matrix $A$ a very sparse structure.

The flows are approximated with centered-difference schemes, meaning the only states relevant for the flow of a certain state are its most adjacent neighbors,

giving the matrix a three-diagonal structure. The main diagonal of $A$ then describes the states' impact on themself. The neighboring states in the first dimension are the ones next to the diagonal of $A$. The other bands contain information from the closest states in the second dimension. The size of the first dimension therefore sets the distance between the bands. An example of the structure of the system matrix is given in figure 5.

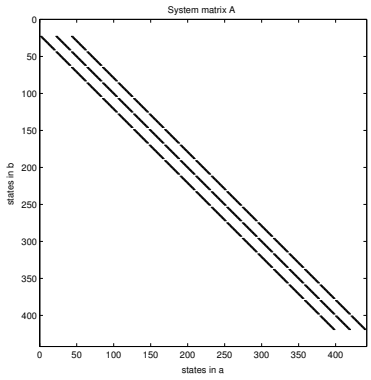


Figure 5: The figure shows the structure of the system matrix A for a two-dimensional system with 21 defines states in each direction. No flows are calculated for the boundary states, introducing zeros in the diagonal.

## 4.4 Probability distribution

The program constructed for performing the linear noise approximation has an iterative structure and the system matrix $A$, the concentration vector $\bar{\phi}(t)$ and the distribution $\Pi(\bar{\xi}, t)$ are calculated at every time-step.

To solve the regular Fokker-Planck equation, $A$ is determined once for all times-steps since it involves only constant coefficients. There is also no need for solving the concentration separately, as mentioned before. This makes it possible to calculate $A$ and a chosen start-distribution and thereafter use a numerical solver, preferably a backward difference solver (BDF) to iterate over all time-steps. In the linear noise approximation, the distribution is solved using a time-dependent $A$ and the concentration vector at every time-step, with the same BDF method:

$$\frac{3}{2}p(t_{k+1}) = 2p(t_k) - \frac{1}{2}p(t_{k-1}) + \Delta t f(p(t_{k+1})) \tag{16}$$

where $f(p) = \frac{d}{dt}p$. This method is an implicit numerical method where $f(p(t_{k+1}))$ depends on the unknown $p_{k+1}$. It is a multi-step method and these methods have stability properties that make them particularly suitable for solving stiff equations which is the case here [5]. Since it is a multi-step method, it includes first taking one step from the start value with an alternative method to find the value at the first time-step. Thereafter the BDF method can begin, using the two former time-steps. Here the alternative method used first is the Euler backwards method:

$$p(t_{k+1}) = p(t_k) + \Delta t f(p(t_{k+1})) \tag{17}$$

The accuracy of our BDF method is of order two while Euler backwards is only of order one.

In matrix formulation, the equations above are written:

| | |
|---|---|
| Euler Backwards | $(\mathbf{I} - \Delta t\mathbf{A})p_{k+1} = p_k$ |
| BDF | $(\frac{3}{2}\mathbf{I} - \Delta t\mathbf{A})p_{k+1} = 2p_k - \frac{1}{2}p_{k-1}$ |

For both methods, the system of equations generated is solved with the backslash operator in MATLAB.

## 4.5 Ordinary differential equations

The probability distribution of the noise in the system is computed with help of the system matrix $A$ and a BDF method. But what about the deterministic parts (13)?

The separation of the differential and stochastic equations does not mean that they are independent of each other, only that they operate on different scales. The probability flows, building up the system matrix $A$, are time-dependent in the regard that they partly consist of mean concentration values, see table 4 in appendix B. This means that solving the differential equations has to be done together with the system matrix $A$ and the calculation of the distribution $\Pi$, as shown in figure 4.

At every timestep the mean concentrations are calculated using the same numerical BDF method as used for the distribution. The equations are non-linear for $\phi$ and therefore solved using Newton's method [5]. The differential equations for both systems used in this project are given in appendix A.

# 5 Results

To start with, the Fokker-Planck equation for the two-dimensional problem was solved numerically, to use as a reference. The focus in this project lied however on solving systems numerically with the linear noise approximation. This was performed on one two-dimensional problem and one four-dimensional, both of them described in detail in appendix A. First, a table of the reached steady state values is presented, both for the LNA and the Fokker-Planck approximation.

Table 3: Steady state concentrations reached for the three different simulations performed. The values from the Fokker-Planck solution is estimated from the plot, the other two values are solved from the differential equations.

| system | steady state value |
|---|---|
| Two-dimensional, FP | $\{a, b\} \approx \{30.5, 30.5\}$ |
| Two-dimensional, LNA | $\{a, b\} = \{30.6386, 30.6386\}$ |
| Four-dimensional, LNA | $\{a, b, e_a, e_b\} \approx \{30.44, 30.44, 4.96, 4.96\}$ |

The steady state value for the Fokker-Planck calculation was approximated from the distribution reached. The values from the LNA calculations were computed from the differential equations.

## 5.1 The Fokker-Planck solution

The numerical solution for the two-dimensional problem, had been performed earlier [1]. Therefore the behavior of the distribution over time and the steady state values of the system for the Fokker-Planck approximation were known. The same distribution and steady state values were obtained here.

The probability distribution of the molecular species involved, $A$ and $B$ is shown in figure 6. Nine time-points were chosen to display the time-evolution of the distribution. The time evolution of the distribution was computed until the change between the distribution in each time-step was less than $10^{-6}$, then the steady state value had been reached. The state space consisted of $100 \times 100$ states, here approximated with $100 \times 100$ grid-points, and the time-step used in the iteration was 1 s. The relatively high number of grid-points was chosen to give a detailed solution of the FP approximation.

The distribution is clearly symmetric and it is located around the steady state value approximated to $\{a, b\} = \{30.5, 30.5\}$. The bent distribution reflects the nonlinear dependences between the two variables.

## 5.2 LNA

The goal for the project was perform linear noise approximations on systems already solved by the Fokker-Planck equation and compare the results. This was done with two different systems and both showed results that were expected.

### 5.2.1 Two-dimensional system

Solving the same two-dimensional problem using LNA, the mean concentration vector and the probability distribution of the noise were calculated separately.

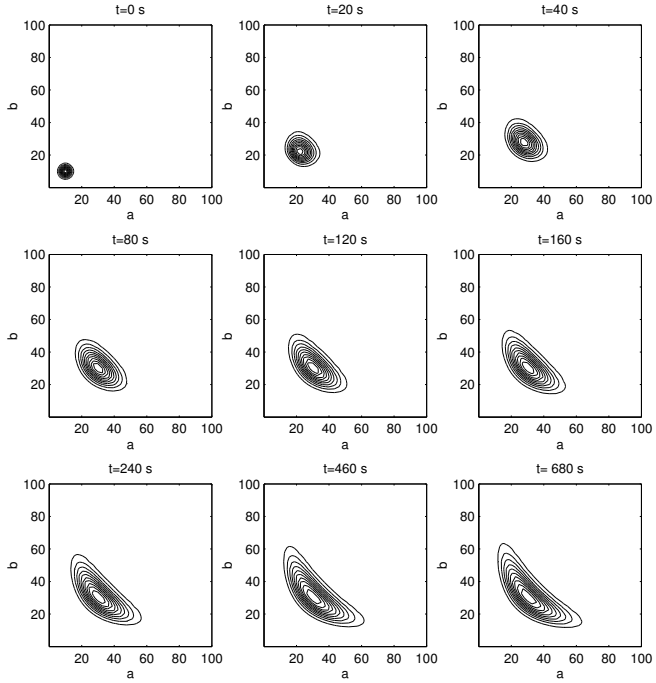


Figure 6: The probability distribution of the two-dimensional problem solved with Fokker-Planck approximation. Number of grid-points used was 100 for 100 states, distributed exponentially. Time-step 1 s with the BDF solver until the change of the distribution between each time-step was less than $10^{-6}$ , starting point $\{a, b\} = \{10, 10\}$.

The calculated probability distribution then only contained information concerning the noise and not the macroscopic values. Therefore it was centered around $\{0, 0\}$ and extended into both negative and positive directions. The distribution was however plotted here in the same manner as the Fokker-Planck solution, figure 6, moving with the concentration of the reactants. This was done to simplify the comparison between the results.

The results of the simulated system are presented in figure 7. Nine different time-steps are displayed, giving a view on the movement of distribution over time. The figure shows a simulation with time-steps of length 10 s, and a grid built on $101 \times 101$ grid-points defining $126 \times 126$ states. The whole grid is not presented in the plots, only the area of interest. The simulation was performed up to t=2000 s. Like for the Fokker-Planck simulations, a change less than $10^{-6}$ for the distribution was obtained after approximately 700 seconds of simulation.

The distribution is linear and symmetric, located around the steady state value $\{30.6386, 30.6386\}$, approximately the same as obtained in the Fokker-Planck solution and exactly the same as the one given in [1]. The number of grid-points chosen was lower than for the Fokker-Planck simulation due to the increased computational demands. Solving this problem with the same grid and same time-steps for both approximations took more than 30 times longer for the LNA due to the repeated calculations of $A$, using the same matrix generator as for the FP solver.

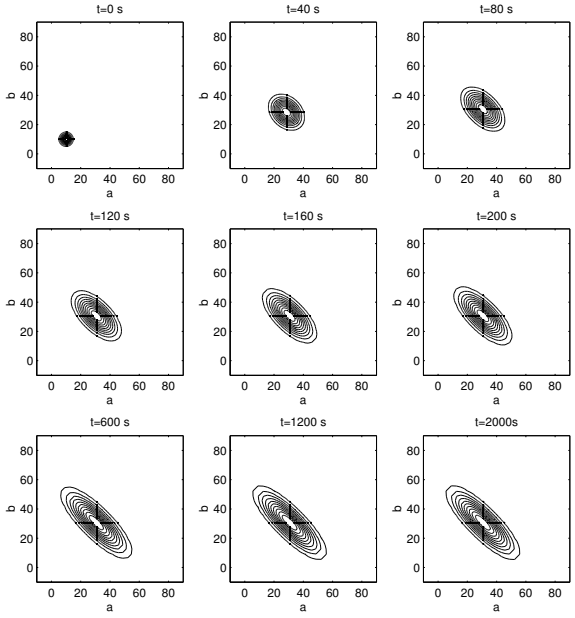


Figure 7: LNA in two dimensions with starting distribution in $\{a, b\} = \{10, 10\}$ and time-step 10 s. Initial mean-concentrations for the enzymes were $\{e_a, e_b\} = \{10, 10\}$. The grid size is 101 grid-points on 126 states, exponentially distributed with maximum density around the steady state value for the stochastic part.

For a closer comparison between the FP and LNA results, steady state distributions from both simulations were plotted together in figure 8.

### 5.2.2 Four-dimensional system

The four dimensional example involves molecules $A$ and $B$ together with $E_A$ and $E_B$, the enzymes involved in the synthesis of $A$ and $B$. The purpose of performing linear noise approximation was to be able to reduce the dimension of the stochastic Fokker-Planck equation. Here the enzymes $E_A$ and $E_B$ were chosen to only be modeled macroscopically, neglecting the stochastics of these variables. The distribution then only displayed the behavior of the molecules $A$ and $B$.

The results of the simulation can be seen in figure 9. The simulation was performed with time-steps 10 s, and grid-size $101 \times 101$ for $126 \times 126$ states. The two-dimensional distribution is linear and symmetric around the steady state value $\{a, b\} \approx \{30.44, 30.44\}$. The steady state value for $A$ and $B$ were slightly different now, compared with the two-dimensional system, but the distribution was still symmetric due to the exact same reactions and parameters for both reactants. The steady state values of the two enzymes, $E_A$ and $E_B$ cannot be read from the plot but were obtained in the calculations to $\{4.96, 4.96\}$. In figure 10, the changes over time for the four different molecular species are presented. Molecules $A$ and $B$ display exactly the same time-evolution due to their identical transition rates. Molecules $E_A$ and $E_B$ also display the exact same behavior for the same reason. The initial values used were $\{a, b, e_A, e_B\} = \{10, 10, 10, 10\}$.

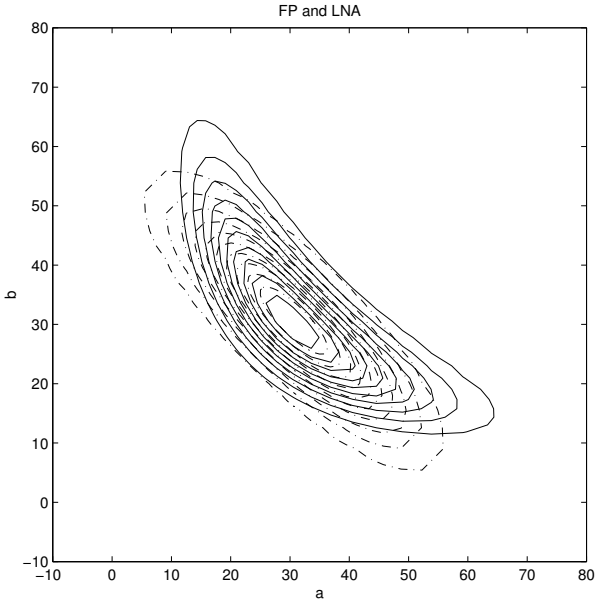


Figure 8: The two-dimensional system solved with the Fokker-Planck approximation, solid lines, and the linear noise approximation, dotted lines. Time-step 10 s and grid-size 101 grid-points for 126 states. Steady state distribution taken at t=1200 s.

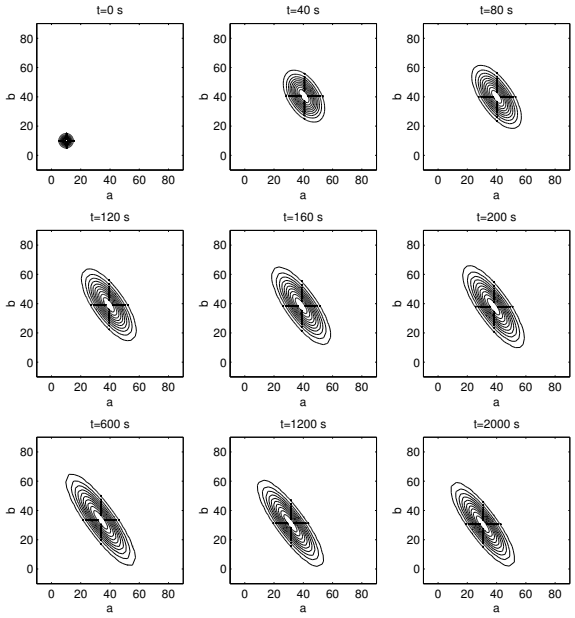


Figure 9: LNA on a four-dimensional problem, with stochastics in only two dimensions, $a$ and $b$. The initial distribution was $\{a, b\} = \{10, 10\}$ and time-step used was 10 s. The grid size was 101 nodes on 126 states, exponentially distributed with maximum density around the steady state value.

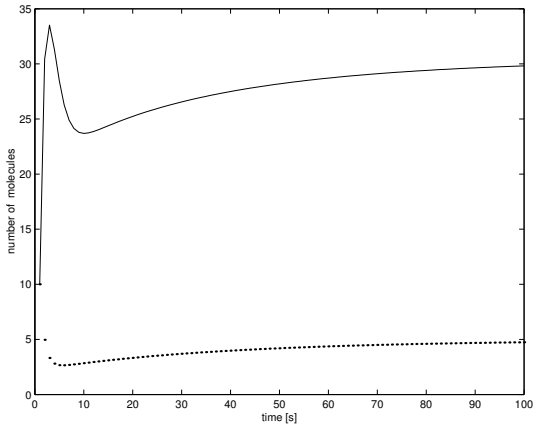


Figure 10: The time-evolution of the number of molecules for the four-dimensional system. Molecules $A$ and $B$ show exactly the same movement, solid line. Likewise, $E_A$ and $E_B$ display exactly the same time-evolution, dotted line. Initial values $\{a, b, e_A, e_B\} = \{10, 10, 10, 10\}$.

The steady state mean concentrations were reached relatively quickly compared to the whole distribution, as seen from figure 10.

## 5.3 Elimination of the fast variable

The calculations using elimination of fast variables were only performed on the two-dimensional problem at steady state. First $V(t)$ was fixed at its quasi-steady state value $V^s(U) = 61.2772$ and $\Pi(\xi_U(V^s), t)$ is calculated, resulting in a Gaussian distribution centered around $U = 0$. The calculations were performed with starting point $U = 3$, timesteps 10 s and the time evolution of the distribution was computed until the change of its norm between each timestep was less than $10^{-7}$. The state space used was 200 states approximated by 120 gridpoints.

The probablity distribution $\Pi(U, V, t)$ was then calculated with the same number of states and gridpoints in the $V$-direction. Also here, the distribution for every $U$-value was computed until the change of its norm between each timestep, dt=10 s was less than $10^{-7}$. The resulting two-dimensional probability distribution was located with its center at $\{u, v\} = \{0, 61.3\}$. In order to better display the result, the distribution was here transformed back to the $AB$-variables. In figure 11 this distribution is plotted together with the Fokker-Planck solution to the same system in order to compare the two results. The distribution from the LNA calculation is no longer linear but follows the curved solution like the Fokker-Planck solution. The agreement between the two methods is good. The former two-dimensional calculation with compexity $N^2$ has here been replaced by two one-dimenional calculations, with total complexity $2N$.

## 5.4 Number of grid-points

To illustrate the impact of the number of grid-points in the grid, a simple comparison was performed. Five different grids with different number of points

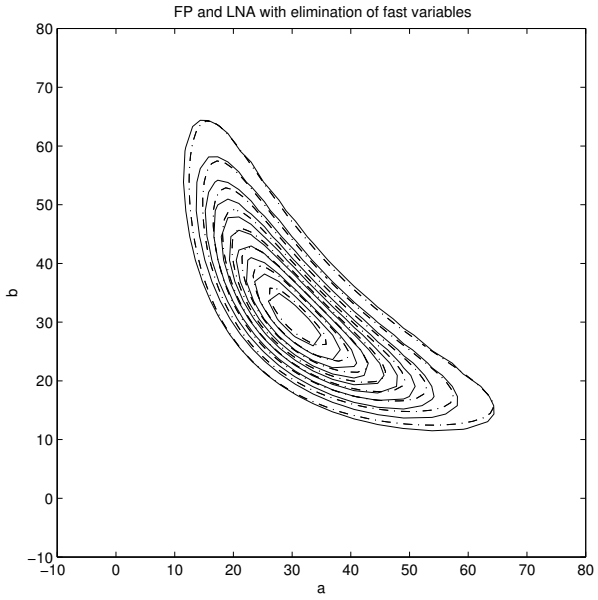


Figure 11: The two-dimensional system solved with the Fokker-Planck approximation, dotted lines, and the linear noise approximation with elimination of the fast variable, solid lines. For the Fokker-Planck calculations a time-step of 10 s and grid-size 101 grid-points for 126 states was used. For the LNA the gridsize was $200 \times 200$ with $121 \times 121$ gridpoints with timesteps of 10 s. The distribution is taken when change is less than $10^{-6}$ for Fokker-Planck, and $10^{-7}$ for LNA.

were constructed. Thereafter the time for calculating the system matrix $A$ and for solving the probability distribution, $p(\mathbf{x}, t)$, using the FP approximation was measured. The system used was the two-dimensional system with molecules $A$ and $B$. Comparison was also done with the linear noise approximation for the same system. For the LNA calculations only 3 grids were tested. The obtained results are presented in figure 12.

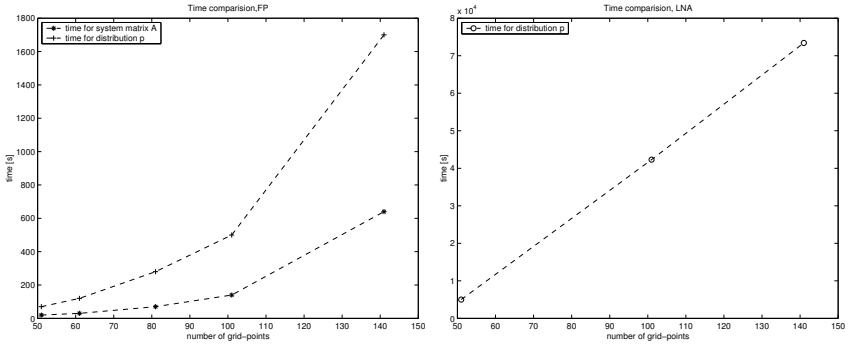


Figure 12: The left figure illustrates the time-change for calculating the system matrix $A$ and the probability distribution $p$ for different grid-sizes, using the Fokker-Planck approximation. The right figure illustrates the time-changes for calculating the probability distribution with different grid-size using LNA. The time is measured after taking 1000 steps with the BDF-solver, time-step 1s.

A doubling of the number of grid-points, from 51 to 101, gave a 7-fold increase in computational time for solving the distribution. This is explained by the increased number of states used in the computations. The increase is approximately the same for both FP and the LNA calculations but the time-costs are much greater to start with in the LNA, $\approx 5000$ s compared to 70 s for the FP-approximation in the present implementation.

# 6 Discussion

## 6.1 Computational demands

The programs constructed here have not been optimized or written in order to be as general as possible. They are created to be able to test whether or not the linear noise approximation, solved with same numerical methods as the Fokker-Planck approximation can give the same or similar results.

There is, as presented in the result section, a significant change in computational time for the LNA compared to the Fokker-Planck approximation. It is therefore quite clear that LNA is a method to use only if the system of interest is too big to solve with any other approximation. The exact computational costs, concerning memory allocation and number of operations performed during the calculations, have not been compared here. But since the two programs are built using the same types of operations, one can assume from the large time differences that the difference in number of operations is rather big. The problem with computational costs can be ameliorated by re-structing the program. One way of improving the speed of the LNA approach is to directly compute the right hand side, $A\Pi$, instead of first computing the matrix $A$ and then multiplying with the probability vector, $\Pi$.

The four-dimensional system mathematically modeled in this project, had been solved using Fokker-Planck by Sjöberg, but larger systems are to my knowledge not computed numerically, either with LNA or Fokker-Planck. What is clear now is that LNA is possible to use numerically with larger systems and it can therefore be used as a tool to describe more complicated systems in the future.

## 6.2 Obtained results

A four-dimensional problem has here been well approximated by a problem of two dimensions, derived by LNA, and further on was the two-dimensional problem replaced by two one-dimensional problems using different timescales in the system. The results obtained for the linear noise simulations were in agreement with what could be expected. Since it is a linear approximation, the former bent distribution for the two-dimensional problem is changed into a linear form. This is of course a drawback of this method but if the computational difficulties for high dimensionality problems are to be overcome, maybe this is a necessary sacrifice to make.

Whether or not the LNA is a good approximation for a system is not always possible to know beforehand. The system volume $\Omega$, is of great importance since a small volume does not justify the removal of equation terms of order $\Omega^{-\frac{1}{2}}$ or lower. Also there can be areas of non-linear dynamics in a system and if the approximation is applied then it will not give an accurate solution [8].

The simplest way to see if the LNA is good for the system of interest is to compare the results with for example a Gillespie simulation of the same system [4]. No such comparisons have been performed in this project but it is necessary if one wants to know exactly how good an approximation LNA can be.

In the four-dimensional problem, $E_A$ and $E_B$ are chosen only to be described macroscopically. When studying the steady state results obtained after the simulation, it is obvious that these two molecules in fact are present in a lower

copy number than $A$ and $B$. However, this simulation was only a test in order to see if it was numerically possible to solve the separated equations. Thus, there is no analysis done on the results obtained from the simulation.

### 6.3 Number of grid-points

The number of grid-points defining the grids have been mentioned as an important factor determining accuracy and computational time. As seen in figure 12 doubling the number of grid-points, from 51 to 101, will lead to approximately a 7-fold increase in calculation time for the distribution $p$ or $\Pi$. When solving the Fokker-Planck equation the system matrix is constant, hence only calculated once. But performing LNA means handling time-dependent coefficients in $A$ needing it to be calculated at every time-step in the present implementation. In these calculations an increase in time costs is clearly notable. It is also of importance to choose a number of grid-points that is sufficient for a smooth probability function but still low enough to save time and operations. In this report there are no comparisons of accuracy between the difference grids, but for further studies with numerical solutions using LNA, the optimal grid-size should be determined in order to avoid unnecessary computational costs.

### 6.4 Future work

The ability to perform numerical LNA calculations is a step towards the mathematical modeling of multidimensional systems stochastically. It is shown in this project that calculations with LNA and its separation of scales give expected results. To further study this approximation it is though necessary to more in detail compare the accuracies of LNA and FP. There have to be studies on the accuracies for different types of systems, since there are differences in the suitability of LNA. It is also of great importance to optimize the programs in order to simplify for larger systems to be studied. The programs and methods used in this project can be re-structured in many ways to decrease the computational costs.

As mentioned before, the calculations in this project assumes spatial homogeneity in the system, something that is not very realistic in cells where reactions sometimes can be restricted to only one location. The boundary conditions used here may also not be optimal for all systems. They are here chosen to be the exact same as in [1] for simplicity.

## 7 Acknowledgments

I would first like to thank my supervisors, Paul Sjöberg and Per Lötstedt for guiding me and kindly helping me with all my questions. I also would like to thank Andreas for supporting me over the phone whenever I was feeling tired and willing to give up. And of course my friends who all questioned why I chose this master thesis project but at least tried to understand my choice and still asked me to go and have coffee with them on breaks. And last, I also would like to say thank you to Steffie who used to tell me that I was smart and could do anything. See you someday!

# References


[1] P. Sjöberg. *Numerical solution of the master equation in molecular biology.* Master's degree project, Dept. of Scientific Computing, Uppsala University, Sweden. 2002

[2] N. G. van Kampen. *Stochastic Processes in Physics and Chemistry.* Elsevier, Amsterdam. 1992.

[3] J. Elf, J. Paulsson, O. Berg, M. Ehrenberg. *Near-critical phenomena in intracellular metabolite pools.* Biophysical Journal, 84:154-170,2003.

[4] J. Elf, M. Ehrenberg. *Fast evaluation of fluctuations in biochemical networks with the linear noise approximation.* Genome Research, 13:2475-2484, 2003.

[5] M. T. Heath. *Scientific Computing - An Introductory Survey*, McGraw-Hill Companies, 1997.

[6] N.A.Campbell. *Biology*, Pearson Education POD, 1996.

[7] J. Paulsson, *The stochastic nature of intracellular control circuits*, licentiate thesis, Dept. of Cell. and Mol. Biol., Uppsala University, Sweden. 2000.

[8] Johan Elf, personal communication.

[9] J. Elf, *Mathematical modelling of bacterial control systems*, licentiate thesis, Dept. of Cell. and Mol. Biol., Uppsala University, Sweden. 2001.

[10] J. Elf, O. Berg, M. Ehrenberg. *Feedback inhibition attenuates deleterious fluctuations in coupled metabolic pools.* Manuscript included in licentiate thesis of J. Elf. 2001.

[11] J. Elf, M. Ehrenberg. *Stoichiometric flux coupling destabilises bacterial protein synthesis.* Manuscript included in licentiate thesis of J. Elf. 2001.

# A Model systems

Here the schemes for the two different models used in this project are presented. There is one two-dimensional model and one four-dimensional. To be able to perform comparison with earlier work done by Paul Sjöberg [1], these systems are the exact same as used in his study.

## A.1 Two-dimensional system

### A.1.1 Reactions

$$\begin{aligned} &\emptyset \xrightarrow{k_0} A && \emptyset \xrightarrow{k_0} B \\ &A \xrightarrow{\mu[a]} \emptyset && B \xrightarrow{\mu[b]} \emptyset \\ &A + B \xrightarrow{k_2[a][b]} \emptyset \end{aligned}$$

where $[a]$ symbolizes the concentration of molecule $A$.

### A.1.2 Deterministic equations

$$\frac{d[a]}{dt} = k_0 - \mu[a] - k_2[a][b] \tag{18}$$

$$\frac{d[b]}{dt} = k_0 - \mu[b] - k_2[a][b] \tag{19}$$

### A.1.3 Constants

$k_0 = 1\ Ms^{-1}$, $k_2 = 0.001\ M^{-1}s^{-1}$, $\mu = 0.002\ s^{-1}$

$k_0$ is the rate of formation for $A$ and $B$. $\mu$ is the cell growth rate, or the rate with which the molecules are diluted. $k_2$ is the rate with which $A$ and $B$ together form a third complex.

## A.2 Four-dimensional system

### A.2.1 Reactions

$$\begin{aligned} &\emptyset \xrightarrow{\frac{k_a[e_a]}{1+\frac{[a]}{K_I}}} A && \emptyset \xrightarrow{\frac{k_b[e_b]}{1+\frac{[b]}{K_I}}} B \\ &A \xrightarrow{\mu[a]} \emptyset && B \xrightarrow{\mu[b]} \emptyset \\ &A + B \xrightarrow{k_2[a][b]} \emptyset \\ &\emptyset \xrightarrow{\frac{k_{e_a}}{1+\frac{[a]}{K_R}}} E_A && \emptyset \xrightarrow{\frac{k_{e_b}}{1+\frac{[b]}{K_R}}} E_B \\ &E_A \xrightarrow{\mu[e_a]} \emptyset && E_B \xrightarrow{\mu[e_b]} \emptyset \end{aligned}$$

### A.2.2 Deterministic equations

$$\frac{d[a]}{dt} = \frac{k_a[e_a]}{1 + \frac{[a]}{K_I}} - \mu[a] - k_2[a][b] \tag{20}$$

$$\frac{d[b]}{dt} = \frac{k_b[e_b]}{1 + \frac{[b]}{K_I}} - \mu[b] - k_2[a][b] \tag{21}$$

$$\frac{d[e_a]}{dt} = \frac{k_{e_a}}{1 + \frac{[a]}{K_R}} - \mu[e_a] \tag{22}$$

$$\frac{d[e_b]}{dt} = \frac{k_{e_b}}{1 + \frac{[b]}{K_R}} - \mu[e_b] \tag{23}$$

### A.2.3 Constants

$k_a = k_b = 0.3\ s^{-1}$, $k_2 = 0.001\ s^{-1}M^{-1}$, $K_I = 60$, $\mu = 0.002\ s^{-1}$, $k_{e_a} = k_{e_b} = 0.02\ Ms^{-1}$, $K_R = 30$

This expanded model contains the concentrations of $E_A$ and $E_B$ also. These are controled through transcriptional repressor control using the parameter $K_r$. $K_r$ indicates the amino acid concentration for which the transcription is half repressed [1]. Procuction of $A$ and $B$ is here controlled with feedback inhibition through the parameter $K_I$. $\mu$ is the dilution rate, and $k_a$,$k_b$,$k_{ea}$, $k_{eb}$ and $k_2$ are reaction rates.

# B Expansion example

## B.1 Two dimensional example

In this section, an example of what the expansion would look like in two dimensions, is given. In the case where the system is two-dimensional, $p$ is a function of two variables plus time, $p(a, b, t)$, and with a change of variables the function $\Pi$ will also be a function of two variables plus time, $\Pi(\xi, \eta, t)$. The example will describe the two-dimensional system in appendix A, involving two metabolites created and consumed through a total of five different reactions.

The linear noise expansion is, as mentioned in the theory, an expansion of the master equation in powers of $\Omega$, the system volume. Each reactant has to be expressed in powers of $\Omega$ as well, and all probability flows are also redefined. This section will simply give an example of this method, not go through any of the equations or the definitions. For the general formulation see section 3.3.1.

The molecules $a$, $b$ and $p(a, b, t)$ written in the new variables:

$$\begin{aligned} a &= \Omega\phi + \Omega^{\frac{1}{2}}\xi \\ b &= \Omega\psi + \Omega^{\frac{1}{2}}\eta \end{aligned}$$

$$p(a, b, t) = p(\Omega\phi + \Omega^{\frac{1}{2}}\xi, \Omega\psi + \Omega^{\frac{1}{2}}\eta, t) = \Pi(\xi, \eta, t) \tag{24}$$

The correlation between the functions $p$ and $\Pi$ is necessary to find in order to rewrite the equations correctly. The function $\Pi(\xi, \eta, t)$ differentiated with respect to $t$ gives,

$$\begin{aligned} \frac{\partial \Pi}{\partial t} &= \frac{\partial p}{\partial t} + \Omega\frac{d\phi}{dt}\frac{\partial p}{\partial a} + \Omega\frac{d\psi}{dt}\frac{\partial p}{\partial b} \\ &= \frac{\partial p}{\partial t} + \Omega^{\frac{1}{2}}\frac{d\phi}{dt}\frac{\partial \Pi}{\partial \xi} + \Omega^{\frac{1}{2}}\frac{d\psi}{dt}\frac{\partial \Pi}{\partial \eta} \end{aligned}$$

or

$$\frac{\partial p}{\partial t} = \frac{\partial \Pi}{\partial t} - \Omega^{\frac{1}{2}}\frac{d\phi}{dt}\frac{\partial \Pi}{\partial \xi} - \Omega^{\frac{1}{2}}\frac{d\psi}{dt}\frac{\partial \Pi}{\partial \eta} \tag{25}$$

Equation (25) describes the relation between the two functions $p$ and $\Pi$ expressed in orders of $\Omega$. To rewrite the master equation we also need to express the probability flows in the new variables according to (7):

$$\begin{aligned} w_r(\mathbf{x} + \mathbf{n_r})p(\mathbf{x} + \mathbf{n_r}, t) &= q_r(\mathbf{x} + \mathbf{n_r}, t) \\ &= \rho_r(\bar{\xi} + \Omega^{-\frac{1}{2}}\mathbf{n_r}, t) \end{aligned}$$

where $\bar{\xi} = [\xi\ \eta]$, the vector containing the stochastic variables, and $\bar{n_r}$ is the vector where the change in $\xi$ or $\eta$ for a certain transition is defined. The probability flows $\rho_r$ are defined in the new variables according to (8) and the transition probabilities $\omega_{rk}$ are described in table 4.

Using the general formula for approximating the master equation presented in (10) gives the total equation for the probability distribution for the two-dimensional system, (26).

Table 4: The table shows the transition probabilities in the linear noise approximation of the two-dimensional system. The two different flows represent the transitions for the two different scales.

| reaction | $n = (n_A\ n_B)$ | former $\omega_r$ | $\omega_{r0}$ | $\omega_{r1}$ |
|---|---|---|---|---|
| $\emptyset \xrightarrow{k_0} A$ | $(-1\ 0)$ | $\Omega k_0$ | $\Omega k_0$ | $0$ |
| $\emptyset \xrightarrow{k_0} B$ | $(0\ -1)$ | $\Omega k_0$ | $\Omega k_0$ | $0$ |
| $A \xrightarrow{\mu[a]} \emptyset$ | $(1\ 0)$ | $\Omega\mu[a]$ | $\Omega\mu\phi$ | $\Omega^{\frac{1}{2}}\mu\xi$ |
| $B \xrightarrow{\mu[b]} \emptyset$ | $(0\ 1)$ | $\Omega\mu[b]$ | $\Omega\mu\psi$ | $\Omega^{\frac{1}{2}}\mu\eta$ |
| $A + B \xrightarrow{k_2[a][b]} \emptyset$ | $(1\ 1)$ | $\Omega k_2[a][b]$ | $\Omega k_2\phi\psi$ | $\Omega^{\frac{1}{2}}k_2(\phi\eta + \psi\xi)$ |

$$\begin{aligned}\frac{\partial\Pi}{\partial t} - \Omega^{\frac{1}{2}}\sum_{i=1}^{m}\frac{d\phi}{dt}\frac{\partial\Pi}{\partial\xi} - \Omega^{\frac{1}{2}}\sum_{i=1}^{m}\frac{d\psi}{dt}\frac{\partial\Pi}{\partial\eta} &= \Omega^{\frac{1}{2}}\sum_r n_{r\xi}\frac{\partial(\omega_{r0}\Pi)}{\partial\xi} + \Omega^{\frac{1}{2}}\sum_r n_{r\eta}\frac{\partial(\omega_{r0}\Pi)}{\partial\eta} \\ &+ \Omega^0\sum_r n_{r\xi}\frac{\partial(\omega_{r1}\Pi)}{\partial\xi} + \Omega^0\sum_r n_{r\eta}\frac{\partial(\omega_{r1}\Pi)}{\partial\eta} + \mathcal{O}(\Omega^{-\frac{1}{2}}) \\ &+ \Omega^0\sum_r \frac{n_{r\xi}n_{r\xi}}{2}\frac{\partial^2(\omega_{r0}\Pi)}{\partial\xi^2} + \Omega^0\sum_r \frac{n_{r\eta}n_{r\eta}}{2}\frac{\partial^2(\omega_{r0}\Pi)}{\partial\eta^2} \\ &+ \Omega^0\sum_r \frac{n_{r\xi}n_{r\eta}}{2}\frac{\partial^2(\omega_{r0}\Pi)}{\partial\xi\partial\eta} + \mathcal{O}(\Omega^{-\frac{1}{2}})\end{aligned} \tag{26}$$

The equation presented above, contains all orders of $\Omega$ over $\Omega^{\frac{1}{2}}$. Since $\Omega$ is a large factor there is however a large scale difference between the different orders. The separation of these scales gives two equations:

$$\begin{aligned}\Omega^{\frac{1}{2}}: \quad 0 = \quad & \frac{d\phi}{dt}\frac{\partial\Pi}{\partial\xi} + \frac{d\psi}{dt}\frac{\partial\Pi}{\partial\eta} \\ & + \sum_r n_{r\xi}\omega_{r0}\frac{\partial\Pi}{\partial\xi} + \sum_r n_{r\eta}\omega_{r0}\frac{\partial\Pi}{\partial\eta} \\ \Omega^0: \quad \tfrac{\partial\Pi}{\partial t} = \quad & \sum_r n_{r\xi}\frac{\partial(\omega_{r1}\Pi)}{\partial\xi} + \sum_r n_{r\eta}\frac{\partial(\omega_{r1}\Pi)}{\partial\eta} \\ & + \frac{1}{2}\sum_r n_{r\xi}n_{r\xi}\frac{\partial^2(\omega_{r0}\Pi)}{\partial\xi^2} + \frac{1}{2}\sum_r n_{r\eta}n_{r\eta}\frac{\partial^2(\omega_{r0}\Pi)}{\partial\eta^2} \\ & + \frac{1}{2}\sum_r n_{r\xi}n_{r\eta}\frac{\partial^2(\omega_{r0}\Pi)}{\partial\xi\partial\eta}\end{aligned} \tag{27}$$

The first equation consists of two differential equations concerning, $\phi$ and $\psi$. They give the macroscopic steady state values for the system. The second equa-

tion, the Fokker-Planck equation for $\Pi(\xi, \eta, t)$, gives the probability distribution for $\xi$ and $\eta$. Since the first equation has to be satisfied for all $\Pi$ we let:

$$\frac{d\phi}{dt} + \sum_r n_{r\xi}\omega_{r0}\frac{\partial \Pi}{\partial \xi} = 0 \frac{d\psi}{dt} + \sum_r n_{r\eta}\omega_{r0}\frac{\partial \Pi}{\partial \eta} = 0 \tag{28}$$

## B.2 Transition flows for four-dimensional system

The four-dimensional system treated in this project, was described with stochastics of only molecule $A$ and $B$. The enzymes $E_A$ and $E_B$ are described only macroscopically but their mean-concentrations over time does affect the stochastic behavior of $A$ and $B$. The transition flows for this system using the linear noise approximation are given in table 5. The stochastic variables are here referred to as $\xi_A$ and $\xi_B$ and all mean-concentration parameters as $\phi$.

Table 5: The table shows the transition probabilities in the linear noise approximation of the four-dimensional system. The two different flows represent the transitions for the two different scales.

| reaction | $n = (n_A\ n_A\ n_{E_A}\ n_{E_B})$ | former $\omega_r$ | $\omega_{r0}$ | $\omega_{r1}$ |
|---|---|---|---|---|
| $\emptyset \xrightarrow{\frac{k_a[e_a]}{1+\frac{[a]}{K_I}}} A$ | $(-1\ 0\ 0\ 0)$ | $\frac{k_a[e_a]}{1+\frac{[a]}{K_I}}$ | $\Omega\frac{k_a\phi_{e_A}}{1+\frac{\phi_A}{K_I}}$ | $-\Omega^{\frac{1}{2}}\frac{k_aK_I\phi_{e_A}\xi_A}{(K_I+\phi_A)^2}$ |
| $\emptyset \xrightarrow{\frac{k_b[e_b]}{1+\frac{[b]}{K_I}}} B$ | $(0\ -1\ 0\ 0)$ | $\frac{k_b[e_b]}{1+\frac{[b]}{K_I}}$ | $\Omega\frac{k_b\phi_{e_B}}{1+\frac{\phi_B}{K_I}}$ | $-\Omega^{\frac{1}{2}}\frac{k_bK_I\phi_{e_B}\xi_B}{(K_I+\phi_B)^2}$ |
| $A \xrightarrow{\mu[a]} \emptyset$ | $(1\ 0\ 0\ 0)$ | $\mu[a]$ | $\Omega\mu\phi_A$ | $\Omega^{\frac{1}{2}}\mu\xi_A$ |
| $B \xrightarrow{\mu[b]} \emptyset$ | $(0\ 1\ 0\ 0)$ | $\mu[b]$ | $\Omega\mu\phi_B$ | $\Omega^{\frac{1}{2}}\mu\xi_B$ |
| $A + B \xrightarrow{k_2[a][b]} \emptyset$ | $(1\ 1\ 0\ 0)$ | $k_2[a][b]$ | $\Omega k_2\phi_A\phi_B$ | $\Omega^{\frac{1}{2}}k_2(\phi_B\xi_B + \phi_B\xi_A)$ |
| $\emptyset \xrightarrow{\frac{k_{e_a}}{1+\frac{[a]}{K_R}}} E_A$ | $(0\ 0\ -1\ 0)$ | $\frac{k_{e_a}}{1+\frac{[a]}{K_R}}$ | $\Omega\frac{k_{e_A}}{1+\frac{\phi_A}{K_R}}$ | $-\Omega^{\frac{1}{2}}\frac{k_{e_A}K_R\xi_A}{(K_R+\phi_A)^2}$ |
| $\emptyset \xrightarrow{\frac{k_{e_b}}{1+\frac{[b]}{K_R}}} E_B$ | $(0\ 0\ 0\ -1)$ | $\frac{k_{e_b}}{1+\frac{[b]}{K_R}}$ | $\Omega\frac{k_{e_B}}{1+\frac{\phi_B}{K_R}}$ | $-\Omega^{\frac{1}{2}}\frac{k_{e_B}K_R\xi_B}{(K_R+\phi_B)^2}$ |
| $E_A \xrightarrow{\mu[e_a]} \emptyset$ | $(0\ 0\ 1\ 0)$ | $\mu[e_a]$ | $\Omega\mu\phi_{e_A}$ | $0$ |
| $E_B \xrightarrow{\mu[e_b]} \emptyset$ | $(0\ 0\ 0\ 1)$ | $\mu[e_b]$ | $\Omega\mu\phi_{e_B}$ | $0$ |

## B.3 Variable change

Performing the variable change for improving the linear noise approximation, changes all the involved reactions and equations for the system. The new deterministic equations, transition flows and stochastic equations for variable $U$ and $V$ are presented here in this section.

The new variables:

$$U = A - B$$
$$V = A + B$$

Changing variables lead to a change in definition of the reactions that occur in the system. The redefined reactions together with the transition flows are presented in table 6.

Table 6: Table of the new rections and there transition flows after performing the linear noise approximation.

| reaction | $\omega_{r1}$ | $\omega_{r0}$ |
|---|---|---|
| $U + V \xrightarrow{\frac{1}{2}\mu([u]+[v])} a$ | $\Omega^{\frac{1}{2}} \frac{1}{2}\mu(\xi_u + \xi_v)$ | $\Omega \frac{1}{2}\mu(\phi_u + \phi_v)$ |
| $V - U \xrightarrow{\frac{1}{2}\mu([v]-[u])} b$ | $\Omega^{\frac{1}{2}} \frac{1}{2}\mu(\xi_v + \xi_u)$ | $\Omega \frac{1}{2}\mu(\phi_v - \phi_u)$ |
| $2V \xrightarrow{\frac{1}{4}k_2(\phi_v^2 - \phi_u^2)} \emptyset$ | $\Omega^{\frac{1}{2}} \frac{1}{2}k_2(\phi_v\xi_v - \phi_u\xi_u)$ | $\Omega \frac{1}{4}k_2(\phi_v^2 - \phi_u^2)$ |
| $\emptyset \xrightarrow{k_0} U + V$ | 0 | $\Omega k_0$ |
| $\emptyset \xrightarrow{k_0} V - U$ | 0 | $\Omega k_0$ |

As disussed in the theory part, the elimination of the fast variable comes from the separation of timescales. The eigenvectors are after the variable change directed along the two variable axes with the fast eigenvector along the $V$-axis. An illustration of the eigenvectors for both the $AB$ and the $UV$-systems are given in figure 13. For further information about the eigenvectors and eigenvalues for the two systems see [10].

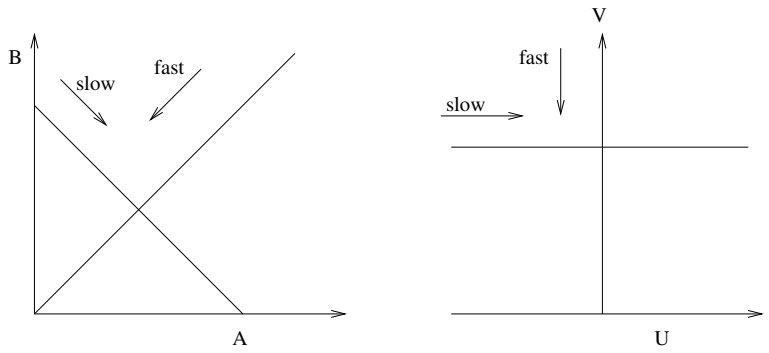


Figure 13: The left illustration shows the $AB$-system with its fast and slow eigenvectors. The right illustration shows the fast and slow eigenvectors for the $UV$-system.

The LNA is performed in one dimension at a time. First for the slow variable $U$ and therafter for $V$, using the information from the distribution of $U$. The differential equations and the stochastic equations for the two variables are presented in table 7.

Table 7: Table presenting the differential and stochastic equations for the two different linear noise calculations.

| | |
|---|---|
| U: | $\frac{d\phi_u}{dt} = -\mu\phi_u$ |
| | $\frac{\partial\Pi(\xi_u,t)}{\partial t} = \mu\frac{\partial}{\partial\xi_u}(\xi_u\Pi) + (\frac{1}{2}\mu\phi_v + k_0)\frac{\partial^2}{\partial\xi_u^2}\Pi$ |
| V: | $\frac{d\phi_v}{dt} = 2k_0 - \mu\phi_v - \frac{1}{2}k_2(\phi_v^2 - \phi_u^2)$ |
| | $\frac{\partial\Pi(\xi_v,t)}{\partial t} = (\mu + k_2\phi_v)\frac{\partial}{\partial\xi_v}(\xi_v\Pi) + \left(k_0 + \frac{1}{2}\mu\phi_v + \frac{1}{2}k_2(\phi_v^2 - \phi_u^2)\right)\frac{\partial^2}{\partial\xi_v^2}\Pi$ |

# C Numerical approximations

## C.1 Differential approximations

Figure 14 describes the notation for the distances inside the grid and the nodes. (29) to (33) describe the schemes of the central differential approximations used in this project. The weights for second order derivatives differ from the ones in the first order, both described here. The notation $w(x_{ik})$ used here describes the function $w$ for molecule $x_i$ at gridpoint $k$.

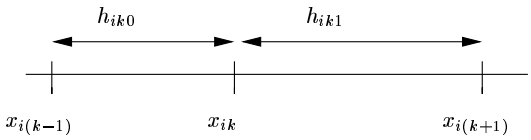


Figure 14: The axis with notations of gridpoints and distances. Index $i = 1, 2 \dots d$, the dimension of the system and index $k = 1, 2 \dots m$ indicates the grid-point's number of dimension $i$.

First derivative in one dimension:

$$\frac{\partial w(x_{ik})}{\partial x_i} = w_{x_i}(x_{ik}) \approx a_{x_{ik}} w(x_{i(k+1)}) + b_{x_{ik}} w(x_{ik}) + c_{x_{ik}} w(x_{i(k-1)}), \tag{29}$$

with weights:

$$\begin{aligned} a_{x_{ik}} &= \frac{h_{ik0}}{h_{ik1}(h_{ik0} + h_{ik1})} \\ b_{x_{ik}} &= \frac{h_{ik1} - h_{ik0}}{h_{ik0} h_{ik1}} \\ c_{x_{ik}} &= -\frac{h_{ik1}}{h_{ik0}(h_{ik0} + h_{ik1})} \end{aligned} \tag{30}$$

Second derivative in one dimension:

$$\frac{\partial^2 w(x_{ik})}{\partial x_i^2} = w_{x_i x_i}(x_{ik}) \approx a_{x_{ik}x_{ik}} w(x_{i(k+1)}) + b_{x_{ik}x_{ik}} w(x_{ik}) + c_{x_{ik}x_{ik}} w(x_{i(k-1)}), \tag{31}$$

with weights:

$$\begin{aligned} a_{x_{ik}x_{ik}} &= \frac{2}{h_{ik1}(h_{ik0} + h_{ik1})} \\ b_{x_{ik}x_{ik}} &= -\frac{2}{h_{ik0} h_{ik1}} \\ c_{x_{ik}x_{ik}} &= \frac{2}{h_{ik0}(h_{ik0} + h_{ik1})} \end{aligned} \tag{32}$$

Second derivative in two dimensions, using the weights from (29):

$$\left.\frac{\partial^2 w(x_{ik},x_{jl})}{\partial x_i \partial x_j}\right|_{i\neq j} = w_{x_i x_j}(x_{ik},x_{jl}) \approx a_{x_{jl}} w_{x_i}(x_{j(l+1)}) + b_{x_{jl}} w_{x_i}(x_{jl}) + c_{x_{jl}} w_{x_i}(x_{j(l-1)}) \approx$$

$$\approx a_{x_{jl}}\Big[a_{x_{ik}} w(x_{i(k+1)},x_{j(l+1)}) + b_{x_{ik}} w(x_{ik},x_{j(l+1)}) + c_{x_{ik}} w(x_{i(k-1)},x_{j(l+1)})\Big]$$

$$+ b_{x_{jl}}\Big[a_{x_{ik}} w(x_{i(k+1)},x_{jl}) + b_{x_{ik}} w(x_{ik},x_{jl}) + c_{x_{ik}} w(x_{i(k-1)},x_{jl})\Big] +$$

$$+ c_{x_{jl}}\Big[a_{x_{ik}} w(x_{i(k+1)},x_{j(l-1)}) + b_{x_{ik}} w(x_{ik},x_{j(l-1)}) + c_{x_{ik}} w(x_{i(k-1)},x_{j(l-1)})\Big]. \tag{33}$$